

## CHARACTERISTIC FEATURES OF GaAs PHOTODETECTOR IN A SEMICONDUCTOR - GAS DISCHARGE STRUCTURE

**B. G. SALAMOV, M. ÖZER, T.S. MAMMADOV**

*Physics Department,*

*Gazi University, Beşevler 06500 Ankara, Turkey*

**S. T. AGALIYEVA**

*National Academy of Science,*

*Institute of Physics,*

*AZ-1143 Baku, Azerbaijan*

Yarımkeçirici-qaz (*SGDS*) struktur funksiyalarını təyin edən, GaAs:Gr sisteminin fotodetektor müqavimət paylanmasıından şüalanma dərəcəsinin stabilisi fiziki prosesləri öyrənilmişdir. Dərəcənin fəza stabililiyinin həyəcanlanması qaz boşalma aralığında həcm boşalması ilə əlaqədardır. Boşalma fəza stabililiyinin mexanizmi fotodetektorda rəqslərin yaranmasına göstərir. Boşalma stabilisiyi fotodetektorun səthinin şüalanmanın udulmasına olan həssaslığından asılıdır.

Изучены физические процессы определяющие функции полупроводника – газовые структура (*SGDS*), стабильность разряда свечения от распределения сопротивления фото детектора системы *GaAs:Cr*. Возмущение пространственной стабильности разряда определено объемным разрядом в газовом разрядном промежутке, которое вызывает значительное искажение электрического поля. Механизм пространственной стабилизации разряда приводит к развитию текущих колебаний в фотодетекторе. Стабильность разряда в основном зависит от чувствительности поверхности фотодетектора к поглощению излучения испускаемое в разрядном промежутке эффективной поверхностью фотодетектора рекомбинационной скоростью, от присутствие окиси и нарушенного поверхностного слоя фотодетектора.

The physical processes that determine the functions of semiconductor - gas discharge structure (*SGDS*), and especially the Townsend and glow-discharge stabilization by the distributed resistance of a *GaAs:Cr* photodetector in such a system are studied. The disturbance of spatial stability of the discharge is determined by the bulk charges in the gas discharge gap that cause a considerable distortion of electric field. The mechanism of spatial stabilization of the discharge involves the development of current fluctuations in the photodetector. It depends strongly on the sensitivity of the photodetector surface toward the absorption of radiation emitted by the discharge gap, the effective surface recombination velocity and on the presence of an oxide or disturbed layer at the interface between the photodetector and the gas discharge plasma.

### 1. INTRODUCTION

The semiconductor - gas discharge structure with a plasma–semiconductor interface as the current conductor was first used in a *SGDS* with a GaAs detector<sup>1</sup>. In this type of *SGDS*<sup>2</sup>, the plasma–semiconductor electrical contact plays a significant role in the treatment of the surface at the interface. The *SGDS* has rather stable operation for a broad range of discharge currents and the current density is stationary and homogeneous over the whole planar structure when an electrically homogeneous cathode is used. Using planar gas discharge cells with a photosensitive *GaAs:Cr*, *GaAs:Zn*, *Si:Zn*, *Si:Pt* photocathode<sup>3,4</sup>, devices for transformation and recording of the *IR* image, on *SGDS* as they are called, have been developed. A high sensitivity of up to  $\lambda = 3 \mu\text{m}$  for *Si:Zn* and  $\lambda = 10.6 \mu\text{m}$  for *Si:Cu* is obtained at 95 K<sup>4</sup>.

In this article, we consider the problem of optimal control and spatial stabilization of one of the simplest gas discharge systems, which is semiconductor gas discharge device initially designed for the conversion of *IR* images to the visible range of light. The CVC of the *SGDS* have been studied in the wide range of pressure, interelectrode distances and conductivities of the *GaAs* photocathode. Moreover, the discharge is accompanied by a short-wave discharge light emission (*DLE*). The results obtained can be used in applications of semiconductor gas discharge devices, such as fast converters of *IR* images<sup>4</sup>, and in the development of pulse sources of light<sup>5</sup>.

### 2. EXPERIMENTAL

Scheme of the *SGDIC* with a *GaAs* photocathode is shown in Fig.1. The total current through the discharge cell and the voltage drop between the electrodes is recorded simultaneously. The diameter of the high-resistivity ( $\rho \sim 10^8 \Omega\text{cm}$ ) *GaAs:Cr* photocathode is 36 mm and its thickness is 1 mm. The outer surface of the wafer is covered with a thin *Au*-film that is transparent to *IR* light.

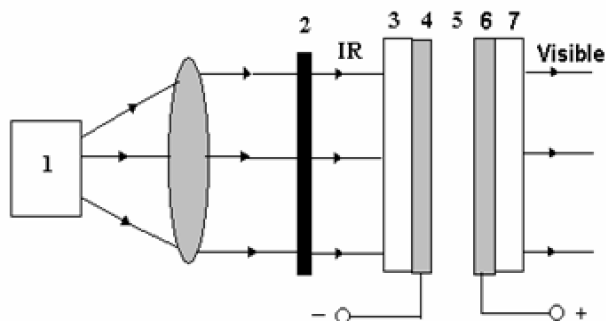


Fig. 1 Scheme of the cell in *SGDS*: 1, light source; 2, *Si* filter; 3, semi-transparent *Au* layer; 4, *GaAs* cathode; 5, gas discharge gap; 6, semi-transparent *SnO<sub>2</sub>* conductor; 7, flat glass disc.

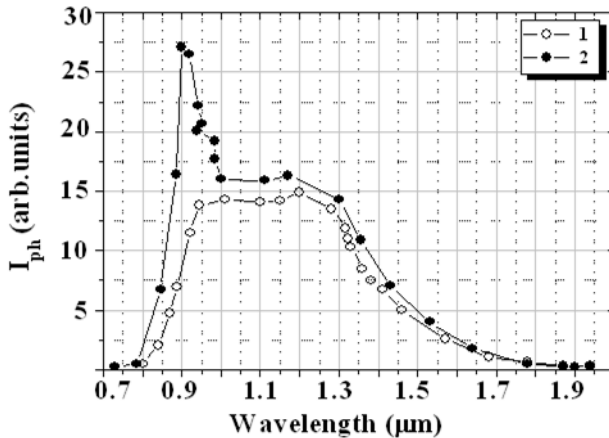


Fig. 3 Spectral characteristic of *GaAs* detector longitudinal photoconductivity, when the light direction coincides (curve 1) and is opposite (curve 2) to field direction.

The second electrode is a glass plate onto the interval surface of which a  $SnO_2$  conductive film is deposited. Such a film is transparent to the visible light. When the amplitude of feeding voltage  $U_0$  exceeds the ignition potential of gas discharge in the gap  $d$ , the gap becomes conductive and some current establishes in the device. Variation of insulator thickness makes it possible to vary the size of the interelectrode air gap  $d$  between 26  $\mu m$  and 4.5 mm. We fixed a certain inter-electrode distance  $d$  and then, for various gas pressures (16 - 760 Torr), measured the breakdown voltage  $U_B$ . A *Si* filter is used to allow the wavelength range  $0.8 \mu m < \lambda < 1.7 \mu m$  for the functioning of *GaAs* photoconductivity. Due to the internal photoeffect, the specific conductivity of the cathode can be manipulated by irradiating with light. When the light is absorbed by the cathode, electrons from the valence band are excited into the conduction band. Hence, the specific conductivity is raised. On the other hand, the feeding voltage  $U_0$  can be changed easily in the experiments.

### 3. RESULTS AND DISCUSSION

Figure 2 give detailed information regarding electrical breakdown in a homogeneous dc electric field and range of stable discharge glow (*SDG*) in the wide pressure range up to atmospheric pressure. The *CVC* allow us to determine the cell parameters: 1) breakdown voltage  $U_B$ ; 2) variation of conductivity  $\sigma$  (or resistivity  $\rho$ ) homogeneities of the photocathode at different illumination intensities  $L$  (*i.e.* change of  $\sigma = \partial j / \partial U$ , or  $\rho = \partial U / \partial j$  where  $j$  is the current density). The value of  $\sigma_{sem} \approx 10^{-8} (\Omega cm)^{-1}$  is determined from the measured *CVC* of the system which is very close to a linear curve when  $U > U_B$ . The shaded area shows the expanded range of *SDG*.

In the case of high resistivity of a *GaAs* cathode the ionizing effect of the active components of the discharge on the cathode, and consequently low density of equilibrium carriers and photocarriers, the generation of carriers in a photocathode under the influence of a gas-discharge plasma play important role<sup>6</sup>. This carrier generation occurs in a very thin skin layer (short - wavelength radiation, about 100 eV electrons and ions). The carriers, aided by the field, then penetrate deep into the interior of the photocathode, where

they can modulate the conductance. The following process resulting in a local increase of current value. Modulation of the bulk of the photocathode and a reduction in its resistance increase the current in the plasma and consequently leads to increase of *DLE* intensity and the flux of the ionizing particles, which in return decrease the resistance of the photocathode to a greater degree. Continuation of this process, which could be regarded as a positive feedback loop, gives rise to *S*-shaped *CVC* of the photocathode and of the current density in one or several local regions on the surface separating the photocathode from the discharge gap. It manifests itself by spontaneous contraction of the *DLE*, initially distributed uniformly over the whole area then into a narrow region. Thus, the filamentation was primarily due to the formation of a space charge of positive ions in the discharge gap, which changed the discharge from the Townsend type to the glow type<sup>6</sup>.

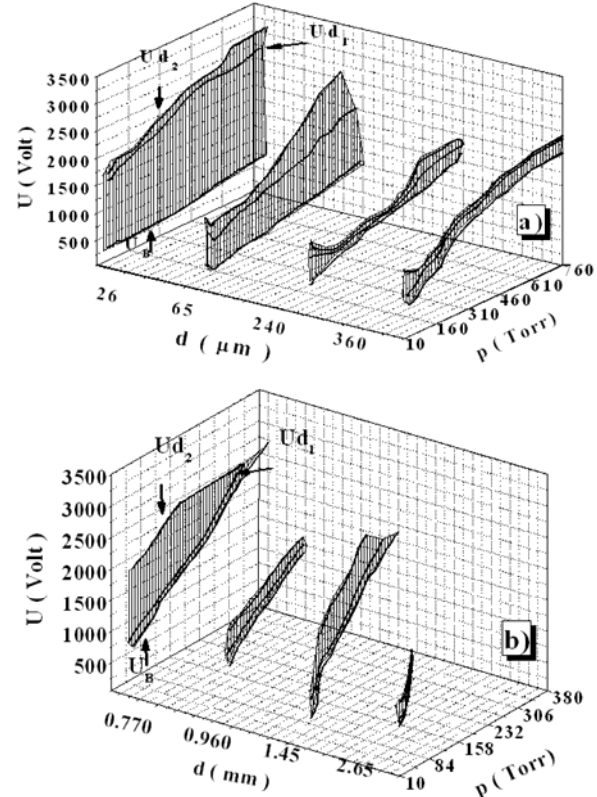


Fig. 2 Regions of *SDG* for the resistances  $R_1$  and  $R_2$  of a *GaAs* photocathode under weak and maximum illumination intensities  $L_1$  and  $L_2$ , respectively. Curves  $U_{d1}$  and  $U_{d2}$  correspond to different voltage, at which the *SDG* is disturbed.

The spectral characteristics of the photocurrent  $I_{ph}$  in a *GaAs* plate with two metallic *Au* contacts for parallel ( $E \uparrow \uparrow L$ ) and opposite ( $E \downarrow \uparrow L$ ) field to the direction of light are shown in Fig. 3 (curves 1 and 2 respectively). A considerable difference of  $I_{ph}$  is observed for  $\lambda < 1.0 \mu m$ . It can be seen from Fig. 4 that in the ( $E \downarrow \uparrow L$ ) field the ratio  $I_{ph}/I_{ph+}$  is higher than in the ( $E \uparrow \uparrow L$ ) field<sup>7</sup>. This fact indicates that the majority of nonequilibrium carriers of the  $I_{ph}$  in the considered *SI GaAs* are electrons. In the range of 0.9 - 1.8  $\mu m$  the photoconductivity in *GaAs:Cr* is attributed to chrome impurities. At the same time in the range of 0.74 - 0.83  $\mu m$

the spectral characteristics of  $I_{ph}$  when a *GaAs* plate in a gas discharge cell is illuminated from the side of a gas discharge plasma is 1.5 - 2 times higher as compared to  $I_{ph}$  when *GaAs* plate is illuminated from the side coated with *Au* layer. In this case the light is absorbed in a narrow ( $10^{-4}$  -  $10^{-5}$  cm) photodetector layer and therefore the observed effect can be explained by a different velocity of surface recombination. At the same time, in the range of 0.74 - 0.83  $\mu\text{m}$  the photocurrent, when a *GaAs* plate is illuminated from the side of a gas discharge plasma, is 1.5 - 2 times higher as compared to photocurrent at the metallic contact illumination. This region (0.74 - 0.83  $\mu\text{m}$ ) for *GaAs* has a large absorption coefficient ( $k = 10^4$  -  $10^5$   $\text{cm}^{-1}$ ). In this case the light is absorbed in a narrow ( $10^{-4}$  -  $10^{-5}$  cm) photodetector layer and therefore the observed effect can be explained by a different velocity of surface recombination.

Thus the increase in longitudinal photoconductivity of a detector on plasma contact, can be explained by decrease of the surface recombination velocity of nonequilibrium carriers in the photodetector, when it is in contact with the gas discharge plasma<sup>8</sup>. The observed phenomenon can be attributed to the change of recombination processes due to bombardment of the detector surface by the charged plasma particles. It should be noted that during the illumination of the *GaAs* through the plasma contact the observed increase in  $I_{ph}$  cannot be attributed to additional illumination by the gas discharge itself. Thus, we have shown that due to the interaction of the active components of the plasma with the detector surface, the photoconductivity increases in the range of strong absorption. First of all, the contacts should be ohmic. Secondly, the transit time  $t_{tr}$  for the minority carries to travel across the sample should be less than the carrier lifetime  $\tau$ . The transit time is given by

$$t_{tr} = L_2 / (\mu_{dr} U) \quad (1)$$

where  $L$  is the distance between the contacts,  $\mu_{dr}$  is the drift mobility and  $U$  is the applied voltage. If an illuminated semiconductor cathode plate of thickness  $L$  is subjected to a voltage  $U$ , the initial photocurrent is

$$I_1 = G\tau(\mu_n + \mu_p) eU (S/L) \quad (2)$$

where  $G$  is the rate of photocarrier generation,  $\mu_n$  and  $\mu_p$  are the electron and hole mobilities and  $S$  is the cross-sectional area of the cathode.

If the applied voltage is such that  $t_{tr} < \tau$ , the minority carriers are extracted from the cathode and they participate in the conduction process only during the transit time. Consequently, the photocurrent begins to fall and, after a time  $t_{tr}$ , it is given by

$$I_2 = G\tau(\mu_n + \mu_p) eU (S/L) = G(1 + \mu_p/\mu_n) eSL \quad (3)$$

i.e. the steady-state or saturation current is independent of the applied voltage. Since the minority carriers are extracted at a constant rate, the transition from  $I_1$  to  $I_2$  is linear.

The quantum efficiency of the formation of the transient process in our system may be much larger than unity because of the effective photoelectric gain in the semiconducting cathode. The quantum efficiency in our system is defined as the ratio of the number of atoms  $N$  to the number of light

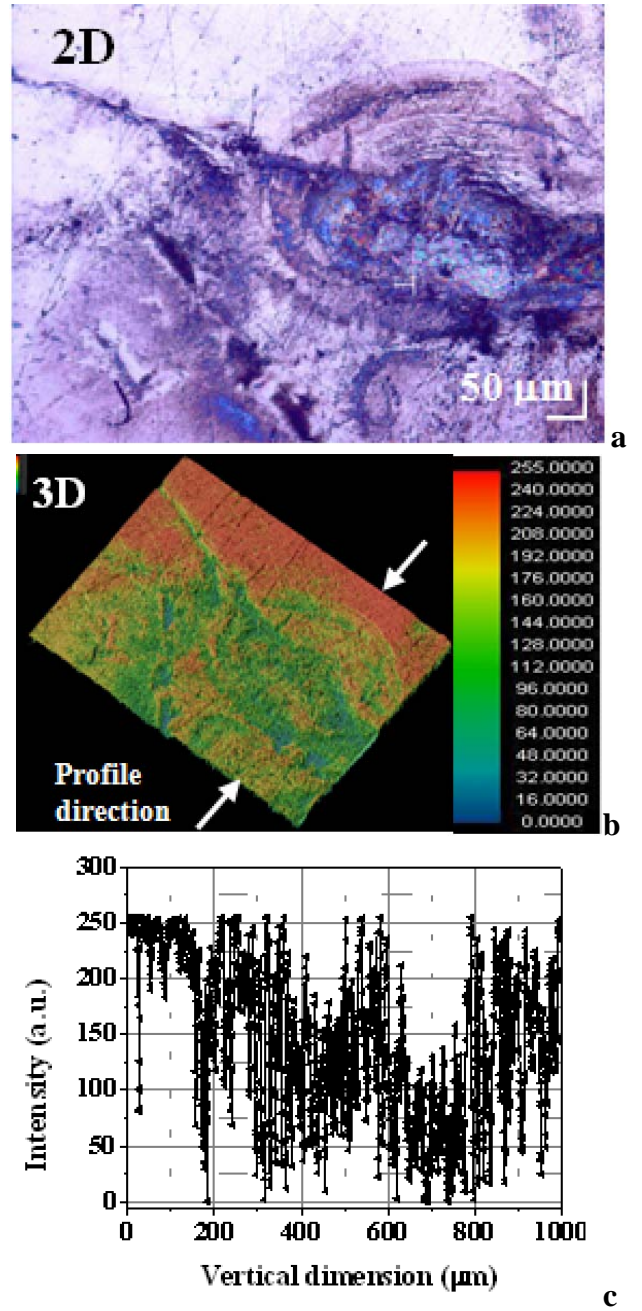


Fig. 4 (a, b, c) 2D and 3D surface pattern of damaged *GaAs* and variation of DLE intensity profile (i.e. gray levels) from indicated direction at 620 Torr.

quanta absorbed, both of which are taken per unit area. Quite general assumptions lead to the following relationship between  $N$  and the duration of exposure  $t_0$ :

$$N = (1/q) DI t_0 \quad (4)$$

where  $I = kJL$  is the number of quanta absorbed per unit time in a layer whose surface area is 1  $\text{cm}^2$ ,  $q$  is the valence of the ions and  $D$  is the photoelectric gain, which is given by the following formula in the case of a simple ambipolar photoconductor:

$$D = (\mu_n + \mu_p) \tau U / L_2 = \tau (1/t_n + 1/t_p) \quad (5)$$

Here,  $\tau$  is the carrier lifetime,  $U$  is the applied voltage,  $L$  is the thickness of the semiconductor plate and  $\mu_n$ ,  $t_n$ ,  $\mu_p$  and  $t_p$ , are, respectively, the mobilities and transit times of electrons and holes. The quantum efficiency of the process may be increased by raising the applied voltage to the limit set by the appearance of a dark unipolar injection current<sup>9</sup>. Estimates for semi-insulating *GaAs* show that the photoelectric gain should be a few tens. The expression obtained demonstrates that the sensitivity of a system with a strongly absorbing semiconductor can be increased effectively by reducing the thickness of the semiconductor and by using uniform weakly absorbed background illumination.

Moreover, paper deals with the influence of interface between *GaAs* cathode, dielectric spacer and conductive *SnO<sub>2</sub>* anode on the space charge formation and electrical breakdown. It is well known that when a dc voltage is applied to insulators, a space charge is formed and the internal electric field is distorted, which affects the breakdown characteristics. However, much is still unclear about the way in which space charge formation is influenced by the *GaAs* cathode, and by the interface between such cathode and the insulator. This *GaAs* layer is very significant in terms of electrodes performance (see Fig.4), and therefore it is important to investigate how space charge formation inside insulators is influenced by the interface with the *GaAs*.

cathode. The effect of the dielectric spacers on the intensity of both the current and the *DLE* may be discussed in term of plasma-surface interactions<sup>10</sup>. Comparison between the thermal bonding and mechanical contact cases suggests that the latter promotes easier formation of space charge<sup>11</sup>. Thus, space charge formation depends on the properties of the interface between the photocathode, and the dielectric spacer.

#### **4. CONCLUSION**

Hence, the two-layer photoconductor – plasma cell considered here is a converter, transforming and amplifying a relatively low-powered photon flux incident on the receiving surface of the photo-detector into a flux of high energy particles, i.e. electrons, ions and photons<sup>12</sup>. Filamentation in the discharge deteriorates the properties of *SGDS* and resolution of the *IR* images. The electronic processes in this two-layer cell are controlled by the properties of the photocathode and the gas-discharge-plasma layer. The results obtained can be used to improve the output characteristics of *SGDS* with a *GaAs* photodetector in the wide pressure range up to atmospheric pressure.

**ACKNOWLEDGMENTS:** This work is supported by DPT2001 K120590 and Gazi University BAP Research Projects 05/2005-53, 05/2006-12, 05/2006-05.

- 
- [1]. *B.G. Salamov*, J. Phys. D: Appl. Phys. 37, 2496 (2004).
  - [2]. *B.G. Salamov*, Infrared Phys. & Technology, 44, 243 (2003).
  - [3]. *B.G. Salamov, K. Colakoglu and S. Altindal*, Infrared Phys. & Technology, 36, 661 (1995).
  - [4]. *Y.A. Astrov, L.M. Portsel*, Sov. Phys. Tech. Phys., 74, 2159 (1993).
  - [5]. *N. Soulem, B. Held*, Eur. Phys. J. AP. 3, 219 (1998).
  - [6]. *B.G. Salamov, S. Buyukakkas, M. Ozer, K. Colakoglu*, Eur. Phys. J. AP. 2, 275 (1998).
  - [7]. *A.P. Goodman*, J.Appl.Phys.30,142 (1958).
  - [8]. *B.G. Salamov*, Imaging Sci. J. 46, 9 (1998).
  - [9]. *Rose*, Helv. Phys. Acta 30 242 (1957)
  - [10]. *J. Sandoval, G. Paez and M. Strojnik*, Optical Eng. 42(12) 3517 (2003).
  - [11]. *Y. Li, T. Takada*, Trans. IEE Japan, IEEE Electrical Insulation Magazine 10(5) 16 (1994).
  - [12]. *L.M. Portsel, Y.A. Astrov, I. Reiman, E. Ammelt, H.-G. Purwins*, J.Appl.Phys. 85, 3960 (1999).

*Daxil olunub: 01.07.2007*